An Analytical Free Energy and the Temperature−Pressure Superposition Principle for Pure Polymeric Liquids

Junhan Cho*

Polymer Science and Engineering Department, Dankook University, San-8 Hannam-dong Yongsan-gu, Seoul 140-714, Korea

Isaac C. Sanchez

Chemical Engineering Department, University of Texas at Austin, Austin, Texas 78712

Received December 8, 1997; Revised Manuscript Received May 7, 1998

ABSTRACT: Recently, it was found that polymers follow the principle of temperature−pressure ($T-P$) superposition. This principle states the temperature insensitiveness of the shape of the configurational free energy. An analytical free energy for polymeric liquids is developed in the framework of the perturbation theory to provide a better understanding of the $T-P$ superposition principle. The intermer potential is separated into the repulsive reference and the attractive perturbed parts. The hard sphere potential is taken as the repulsive reference. The attractive part of the Mie (p,6) potential is taken as the perturbation. The free energy for the reference system of hard chains is obtained from the integration of the hard chain equation of state from the Baxter−Chiew theory. The limiting case of the reference free energy at infinite dilution is derived from the direct evaluation of the configurational partition function. The average packing energy is added as a perturbation energy. The local packing in the nearest neighbor is taken into consideration by the packing energy. The formulated free energy gives a unique interpretation of the empirical $T-P$ superposition principle. The shape of the free energy is shown to be dominantly determined by the packing energy, especially by its (Mie potential) exponents. Therefore, its shape is dominantly temperature insensitive, which is the essence of the $T-P$ superposition principle. In addition, it is shown that the theoretical internal pressure evaluated at atmospheric pressure possesses a maximum at a moderate temperature. At this point, the repulsion in the system starts to dominate the attractive interaction. Some experimental support for this behavior was given in the recent investigations into the bulk data of various polymers. These two features of the model yield the excellent correlation between the experimental and the theoretical polymer bulk properties. Better performance in fitting volumetric data is obtained if a more repulsive potential ($p > 12$) than the Lennard−Jones potential ($p = 12$) is used as a choice of the general Mie potential. This procedure culminates in the prediction of the cohesive energy (CE) of linear polyethylene at room temperature. The model with the Mie (18,6) potential gives the calculated CE within the experimental range, whereas the model with the Lennard−Jones potential overestimates the CE.

Introduction

The volumetric properties of polymer systems are of great importance because the molecular packing and interaction in a given system can be extracted from them. Numerous equations of state, either phenomenological or theoretical, have been suggested to describe this behavior of polymers.[1−14]

Meanwhile, the experimental volumetric data of various bulk polymers were recently reanalyzed in the scaled viewpoint by the present authors.[15−17] The principle of temperature−pressure ($T-P$) superposition was established as a new static property of polymers. The statement of $T-P$ superposition is as follows: a dimensionless pressure variable P/B_0, where B_0 is the bulk modulus B at atmospheric (zero) pressure, is used to superpose compression isotherms into a universal curve. In an alternative statement, the shape of the configurational free energy, which is described by the pressure derivatives of the bulk modulus B, is temperature insensitive. The first pressure derivative B_1 of the modulus implies the asymmetry of the free energy between dilation and compression. Its constancy is the most important in the statement of $T-P$ superposition.

It was shown from the phenomenological argument that B_1 suggests some information on the nature of the interparticle potential.[15,16] The B_1 of salts with strong ionic bonds is 5, due to the symmetry between dilation and compression. Nonpolar polymers with weak van der Waals interaction would be more resistant to compression than to dilation, which tends to increase B_1 from 5. Considering that the $T-P$ superposition principle governs the equation of state properties of polymers, some fundamental questions naturally arise: What are the molecular parameters contributing to B_1? What are the molecular parameters that determine the temperature-insensitive shape of the free energy? These questions, to our surprise, do not seem to have been clearly addressed in the literature. It is, therefore, the main objective of this manuscript to study the molecular interpretation of the $T-P$ superposition principle.

The approach to our goal in this study is to derive and analyze a new analytical equation of state model. At the starting point, the phase space can be described as a continuum or a discrete space. We choose the former. Chains in a continuum enables us to give a more realistic picture of their movements.

The main stream of the continuum approach recourses to the integral equation theory of simple fluids.[18,19] The self-consistent integral equations of the interparticle distribution functions are to be solved for further thermodynamic calculations. Among several

S0024-9297(97)01784-1 CCC: $15.00
Published on Web 08/22/1998

integral equations, the most frequently used is the Percus−Yevick equation.[18,20] It gives an analytical equation of state for the system of hard spheres. Meanwhile, an idealized interparticle potential called the adhesive hard sphere potential was invented by Baxter.[21] This potential possesses the same repulsive core as the hard sphere potential with a strong, but extremely short-ranged attractive interaction tail. The Percus−Yevick equation was directly solved by Baxter for the adhesive hard sphere system to obtain an analytical equation of state.[21,22] This adhesive attractive tail was later utilized by Chiew to build up chains by employing the proper connectivity constraints.[23] A hard chain equation of state was derived in such a way. Other hard chain equations of state were formulated by Wertheim[24−28] and Chapman et al.[29] from the thermodynamic perturbation theory of polymerizing hard spheres with multiple attractive sites. A different and unique work on hard chains was performed by Hall and co-workers[30,31] from generalizing Flory's particle insertion method to its continuum analog.

In this study, the derivation of a new free energy follows the spirit of the perturbation theory.[18,19,32] We separate the total potential in the configurational partition function into a reference and a perturbation. The reference system is simplified to the system of hard chains. The reference free energy is then obtained from the integration of the hard chain equation of state from the Baxter−Chiew theory. In this step, the recent argument by Chan and Dill[33] on the partition function of chain systems is used to derive the free energy at infinite dilution.

We focus on the perturbation to the reference free energy. The conventional first-order approximation to perturbation energy is adopted here. A simple, but the most widely used perturbation energy can be given by the mean field (van der Waals) energy. However, a satisfactory physical interpretation of B_1 is not expected from the van der Waals energy because it is no longer a functional of the interparticle potential. We, therefore, devise a different, yet analytical perturbation energy called the packing energy that is obtained from considering the locally packed dense polymer liquids. The final expression of the complete free energy is then analyzed to interpret the asymmetry number B_1 and the $T-P$ superposition principle.

Derivation of the Free Energy

A proper starting point of this study would be the specification of a model molecule. A model n-mer molecule comprises n spheres attached with chemical bonds. We take the simplest picture of the model molecule. The bond length is exactly the distance between centers of adjacent spheres (i.e., tangent spheres). The bond length vibration is ignored by assuming the infinite spring constant for this mode of vibration. No bond angle potential is assumed. The latter assumption restricts this study to flexible polymer systems. A sphere or a mer of the model chain is treated as an interaction site interacting with others via a spherically symmetric potential.

The system of interest comprises N chains of n-mer having n interaction sites. The partition function Q of the system can be written as

$$Q_{NVT} = \frac{1}{N!I^N\Lambda^{3nN}}Z_N \tag{1}$$

where the symbol I indicates the indistinguishability of a single chain (symmetry number). In this case, I should be 2, implying the complete reversion of chains. The symbol Λ is the thermal de Broigle wavelength. In eq 1, Z_N is the configurational partition function of the system

$$Z_N = \int \mathrm{e}^{-\beta V_N} \prod_{i=1}^{N} \mathrm{d}\{\vec{r}_i\} \tag{2}$$

where V_N is the total potential energy and $\beta = 1/kT$ has its usual meaning. The parenthesis in the dummy variable $\{\vec{r}_i\}$ describes the set of $3n$ coordinates for n interaction sites (n-mer) on each chain.

The total potential V_N is divided into two; one is the intermolecular potential U_N and the other is the intramolecular potential W

$$V_N = U_N + W \tag{3}$$

On the assumptions just given, the intramolecular potential is simplified to have only the nonbonded mer−mer interaction (attractive interaction and repulsive excluded volume interaction) and the bond potential (W^{bond}). The torsional potential is implicitly included in this treatment. Utilizing the pairwise additivity assumption, the total potential can essentially be written as

$$V_N = U_N + W \approx \sum_{\text{nonbonded pairs}} u_{ij}(r) + W^{\mathrm{bond}} \tag{4}$$

where $u_{ij}(r)$ is a given intermer potential between mers separated by r.

On the basis of perturbation theory, the pair potential $u_{ij}(r)$ is separated into the reference $u_{ij}^{(0)}(r)$ and the perturbation $u_{ij}^{(1)}(r)$. At this moment, the separation is arbitrary. The perturbed total potential $V_N^{(1)}$ is defined as the perturbation of all pair interactions

$$V_N^{(1)} \equiv \sum_{\text{nonbonded pairs}} u_{ij}^{(1)}(r) \tag{5}$$

The remaining part of the total potential, $V_N - V_N^{(1)}$, defines the reference total potential $V_N^{(0)}$.

The configurational partition function Z_N in eq 2 can be rewritten as

$$Z_N = \int \mathrm{e}^{-\beta[V_N^{(0)} + V_N^{(1)}]}\, \mathrm{d}\{\vec{r}\}^N \tag{6}$$

Multiplying and dividing the reference configurational partition function, $Z_N^{(0)}$, with only the reference total potential, $V_N^{(0)}$, in the Boltzmann factor lead to the following separation relation of the partition function Z_N

$$Z_N = \int \mathrm{e}^{-\beta V_N^{(0)}}\, \mathrm{d}\{\vec{r}\}^N \frac{\int \mathrm{e}^{-\beta V_N^{(1)}} \mathrm{e}^{-\beta V_N^{(0)}}\, \mathrm{d}\{\vec{r}\}^N}{\int \mathrm{e}^{-\beta V_N^{(0)}}\, \mathrm{d}\{\vec{r}\}^N} \tag{7}$$

$$= Z_N^{(0)} \langle \mathrm{e}^{-\beta V_N^{(1)}} \rangle_0$$

where the subscript 0 implies the ensemble average over

the reference total potential. The logarithm is then taken for both sides.

$$\ln Z_N = \ln Z_N^{(0)} + \ln\langle e^{-\beta V_N^{(1)}}\rangle_0 \tag{8}$$

The basic thermodynamic relationships relate the configurational free energy to the partition function as

$$-\beta A = \ln \frac{Z_N}{N! I^N \Lambda^{3nN}} = \ln \frac{Z_N^{(0)}}{N! I^N \Lambda^{3nN}} + \ln \langle e^{-\beta V_N^{(1)}}\rangle_0 \tag{9}$$

The first term in eq 9 defines the reference free energy $-\beta A_0$

$$-\beta A_0 = \ln \frac{Z_N^{(0)}}{N! I^N \Lambda^{3nN}} \tag{10}$$

The remaining term in eq 9 stands for the perturbation.

To formulate an analytical and tractable free energy, one may need to specify the intermer or site−site potential $u(r)$. We employ the following simplified Mie $(p,6)$ potential

$$u(r) = \begin{cases} u_{\mathrm{HS}} = \infty & r < \sigma \\ u_{\mathrm{Mie}} = \epsilon f_p \left[\left(\frac{\sigma}{r}\right)^p - \left(\frac{\sigma}{r}\right)^6\right] & r > \sigma \end{cases} \tag{11}$$

where σ and ϵ indicate the mer diameter and the potential depth, respectively. The prefactor f_p in eq 11 is defined as

$$f_p = \frac{(p^p/6^6)^{1/(p-6)}}{p-6} \tag{12}$$

The individual site−site potential $u(r)$ is now separated into the reference $u^{(0)}(r)$ and the perturbation $u^{(1)}(r)$. The hard sphere (HS) potential is taken as the reference $u^{(0)}(r)$. The separation of the potential in this study follows the spirit of the hard core version of the Barker−Henderson theory of simple fluids.[34] The reference system is then the tangent hard sphere chain fluid. The perturbed potential at $r > \sigma$ is the Mie potential with the repulsive exponent p, which is more general than the Lennard−Jones potential with $p = 12$. This exponent not only provides flexibility in the repulsion strength, but plays an important role in understanding the phenomenological observation of the $T-P$ superposition, which will be discussed in detail in a later section.

The complete derivation of the free energy in eq 9 is separated into two steps. The first task is to derive the reference free energy $-\beta A_0$ in eq 10. The second task is then to derive the perturbation term in eq 9. We start with the former. There arises, however, the problem of the separation of intermolecular and intramolecular interaction when eq 10 is directly evaluated. This difficulty is circumvented here. From the basic thermodynamic relationships, the reference pressure P_0 from the reference free energy is given as

$$\left.\frac{\partial(-\beta A_0)}{\partial V}\right)_T = \beta P_0 \tag{13}$$

Our reference system is the tangent hard chain fluid. A reasonably accurate equation of state can be obtained from Baxter's elaborate work on the system of adhesive hard spheres[21,22] with the proper connectivity constraints[23,35,36]

$$\frac{\beta P_0}{\rho_{\mathrm{m}}} = \left[\frac{1}{1-\eta} + \frac{3\eta}{(1-\eta)^2} + \frac{3\eta^2}{(1-\eta)^3}\right] - \left(1 - \frac{1}{n}\right)\frac{1+\eta/2}{(1-\eta)^2} \tag{14}$$

where ρ_{m} $(\equiv n\rho)$ is the monomer density. One should refer to the original publications for the derivation of eq 14. A new symbol η in eq 14 is the packing fraction $(\eta = \pi n N \sigma^3/6V)$ of the system. It is notable that eq 14 goes to an ideal gas at infinite dilution.

$$P_0 = \frac{\rho_{\mathrm{m}} kT}{n} + O(\rho_{\mathrm{m}}{}^2) = \rho kT + O(\rho^2) \tag{15}$$

Therefore, the reference free energy A_0 can be obtained as

$$\frac{\beta(A_0 - A^{\mathrm{id}})}{nN} = \int_0^\eta \left[\frac{\beta P_0}{\rho_m} - \frac{1}{n}\right]\frac{\mathrm{d}\eta}{\eta} \tag{16}$$

where A^{id} is the Helmholtz free energy at infinite dilution. Performing the integration yields

$$\frac{\beta(A_0 - A^{\mathrm{id}})}{nN} = \frac{3}{2}\left[\frac{1}{(1-\eta)^2} - \left(1 - \frac{1}{n}\right)\frac{1}{1-\eta}\right] - \frac{1}{n}\left[\ln(1-\eta) + \frac{3}{2}\right] \tag{17}$$

To complete the reference free energy A_0, the A^{id} still needs to be evaluated. We attempt to directly manipulate $Z_N^{(0)}(\rho \to 0)$ at zero density following the general treatment by Chan and Dill.[33] At zero density, each hard chain does not experience other chains. Therefore, the reference total potential $V_N^{(0)}(\rho \to 0)$ can be written as the sum of intramolecular potential only

$$V_N^{(0)}(\rho \to 0) = \sum_{i=1}^{N} \sum_{|j-k|>1} u_{jk}^{(0)}(|\vec{r}_{ii}^{(jk)}|) + \sum_{i=1}^{N} \sum_{j} w_{j,j+1}^{\mathrm{bond}}(\vec{r}_{ii}^{(j,j+1)}) \tag{18}$$

where $|\vec{r}_{ii}^{(jk)}|$ is the distance between the two nonbonded j-th and k-th mers on the i-th chain. The second term in eq 18 is the explicit expression of W^{bond}, where $w_{j,j+1}^{\mathrm{bond}}$ represents the bond potential between two adjacent tangent hard spheres. The $w_{j,j+1}^{\mathrm{bond}}$ is assumed to be infinitely strong. The $Z_N^{(0)}(\rho \to 0)$ term can then be equated to

$$Z_N^{(0)}(\rho \to 0) = \int e^{-\beta V_N^{(0)}(\rho \to 0)}\, \mathrm{d}\{\vec{r}\}^N = \prod_{i=1}^{N}\left[\int e^{-\beta\sum u_{jk}^{(0)}(|\vec{r}_{ii}^{(jk)}|) - \beta\sum w_{j,j+1}^{\mathrm{bond}}(\vec{r}_{ii}^{(j,j+1)})} \prod_{l=1}^{n} \mathrm{d}\vec{r}_i^{(l)}\right] \tag{19}$$

where $\vec{r}_i^{(l)}$ indicates the position of the l-th mer on the i-th chain. Changing the dummy variables in the integral yields

$$Z_N^{(0)}(\rho \to 0) = \prod_{i=1}^{N}\left[\int e^{-\beta\sum u_{jk}^{(0)}(|\vec{r}_{ii}^{(jk)}|) - \beta\sum_j w_{j,j+1}^{\mathrm{bond}}(\vec{r}_{ii}^{(j,j+1)})} \mathrm{d}\vec{r}_i^{(1)} \prod_{l=2}^{n} \mathrm{d}\vec{r}_{ii}^{(1l)}\right] \tag{20}$$

The system volume V can be extracted from each integral. It is because the coordinates $\vec{r}_i^{(1)}$ of the first mer on each chain do not affect the intramolecular potential. Therefore, eq 20 can be simplified to

$$Z_N^{(0)}(\rho \to 0) = V^N q^N \tag{21}$$

where q is the remaining integral given as

$$q = \int e^{-\beta\sum u_{jk}^{(0)}(|\vec{r}_{ii}^{(jk)}|)-\beta\sum_j w_{j,j+1}^{\text{bond}}(\vec{r}_{ii}^{(j,j+1)})} \prod_{l=2}^{n} d\vec{r}_{ii}^{(1l)} \tag{22}$$

The q factor is deeply related to the conformation of an isolated hard chain.

The q in eq 22 does not have temperature dependence. It is because the reference hard sphere potential $u^{(0)}$ and the bond potential w^{bond} take two extreme values (i.e., 0 and ∞). It can be left as an unspecified constant that does not affect any further thermodynamic calculations.

Summarizing all of the derivations just presented yields the following complete reference free energy

$$\frac{\beta A_0}{nN} = \frac{3}{2}\left[\frac{1}{(1-\eta)^2} - \left(1-\frac{1}{n}\right)\frac{1}{1-\eta}\right] - \frac{1}{n}\left[\ln(1-\eta) + \frac{3}{2}\right] - \frac{1}{nN}\ln\frac{V^N q^N}{N! I^N \Lambda^{3nN}} \tag{23}$$

Using the definition of the packing fraction gives the following final expression of the reference free energy

$$\frac{\beta A_0}{nN} = \frac{3}{2}\left[\frac{1}{(1-\eta)^2} - \left(1-\frac{1}{n}\right)\frac{1}{1-\eta}\right] - \frac{1}{n}\left[\ln(1-\eta) + \frac{3}{2}\right] + \frac{1}{n}\ln\frac{6\eta I \Lambda^{3n}}{\pi n \sigma^3 q e} \tag{24}$$

where the transcendental number e appears from Stirling's approximation of $N!$ term in eq 23. This derivation resolves the first task.

The next task is to obtain the perturbation term in eq 9. According to Zwanzig,[32] the perturbation term in eq 9 is equated to the sum of the successive momentum of the perturbed intermolecular potential in the λ-expansion

$$\ln\langle e^{-\beta V_N^{(1)}}\rangle_0 = -\beta\langle V_N^{(1)}\rangle_0 + \frac{1}{2}\beta^2(\langle V_N^{(1)2}\rangle_0 - \langle V_N^{(1)}\rangle_0^2) + O(\beta^3) \tag{25}$$

Equation 25 can be rewritten by using the intermolecular (g_0) and intramolecular (ω_0^{nb}) distribution functions for any nonbonded pair. These functions are well defined in the Appendix. A careful manipulation of these distribution functions yields an expression for the first-order perturbation term $\langle V_N^{(1)}\rangle_0$ in eq 25 as

$$\langle V_N^{(1)}\rangle_0 = \frac{V}{2} n\rho \int d\vec{r}\; u^{(1)}(r)[\rho_m g_0(r) + \omega_0^{\text{nb}}] \tag{26}$$

The subscript 0 again denotes the reference system. One should note that the distribution functions are obtained from the reference total potential. This implies that the configuration of the reference system is used in the averaging procedure. The first-order perturbation energy $\langle V_N^{(1)}\rangle_0$ is the sum of all possible pairs of the perturbed interaction between two nonbonded mers. This term will play a major role in developing a new model.

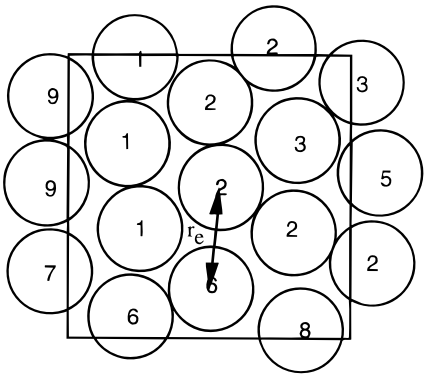

Figure 1. A dense polymeric liquid in 2-dimensional view. The numbers inside the spheres are used to distinguish different chains from others. The symbol r_e represents the most probable distance from the central monomer of interest.

The second-order perturbation term is related to the compressibility of the reference system.[18,34] Our primary concern is polymeric liquids, which are not very compressible. Therefore, we will concentrate on the perturbed free energy by the first-order (Gibbs−Bogoliubov upper limit)[19] in this study. This means that we will minimize the following object function to best fit the experimental bulk data

$$\beta A = \beta A_0 + \frac{V}{2} n\rho\beta \int d\vec{r}\; u^{(1)}(r)[\rho_m g_0(r) + \omega_0^{\text{nb}}] \tag{27}$$

It must be borne in mind that the molecular parameters of polymers obtained from fitting the experimental data are based on the first-order perturbation approximation.

The calculation of the average perturbation energy in eq 27 requires the detailed information on the inter- and intramolecular distribution functions outside the hard sphere diameter. To obtain an analytical equation of state model, we suggest an intuitive approximation to the distribution functions. The usefulness and availability of an analytical theory are the main reasons for this approach. We may also acquire more physical pictures of polymeric liquids from the intuitive approach.

At melt densities, local packing is primarily responsible for compression. A mer on a chain and its nearest neighbor are depicted in Figure 1 (2-dimensional view as an illustration). Intuitively we can measure the average nearest neighbor energy $\langle u\rangle$ as

$$\langle u\rangle = h_z u^{(1)}(r_e) \tag{28}$$

where the distance parameter r_e implies the most probable distance for neighbor mers. The h_z in eq 28 means the number of *nonbonded* mers in the nearest neighbor. The bonded mers should be excluded in eq 28 because of the *correlation hole effect*. This picture of locally packed nearest neighbor is assumed to be smeared into the entire system. The total interaction energy $\langle U\rangle$ would then be

$$\langle U\rangle = \frac{1}{2} nN h_z u^{(1)}(r_e) \tag{29}$$

We call $\langle U\rangle$ in eq 29 the average packing energy.

More detailed mathematical steps give us some clue to the relationship between $\langle U\rangle$ and $\langle V_N^{(1)}\rangle_0$. The total number of nonbonded nearest neighbor mers, h_z, is obtained from the difference between the total number of adjacent mers (the coordination number z) and the number of mers bonded to the central mer

$$h_z \approx \int_0^{r_m} \mathrm{d}\vec{r}\ [\rho_m g_0(r) + \omega_0^{\mathrm{nb}}(r)] = \int_0^{r_m} \mathrm{d}\vec{r}\ [\rho_m g_0(r) + \omega(r)] - \int_0^{r_m} \mathrm{d}\vec{r}\ [\omega(r) - \omega_0^{\mathrm{nb}}(r)] \quad (30)$$

where r_m is the distance corresponding to the first minimum after the first peak in $g_0(r)$. It is the conventional, though not absolute, separation point of the first and second shells. Using eq 30, the perturbation energy can be rewritten as

$$\langle V_N^{(1)}\rangle_0 = \frac{1}{2}nN\int_0^{r_m} \mathrm{d}\vec{r}\ u^{(1)}(r)[\rho_m g_0(r) + \omega_0^{\mathrm{nb}}(r)] + \ldots$$

$$= \frac{1}{2}nN\cdot h_z \frac{\int_0^{r_m}\mathrm{d}\vec{r}\ u^{(1)}(r)[\rho_m g_0(r) + \omega_0^{\mathrm{nb}}(r)]}{\int_0^{r_m}\mathrm{d}\vec{r}\ [\rho_m g_0(r) + \omega_0^{\mathrm{nb}}(r)]} + \ldots \quad (31)$$

In eq 31, only the contribution to $\langle V_N^{(1)}\rangle_0$ from the first coordination shell is explicitly written. The contributions from higher shells are hidden in this equation. We may define a probability density function, $P_1(r)$, only for the first shell as

$$P_1(r) = \frac{\rho_m g_0(r) + \omega_0^{\mathrm{nb}}(r)}{\int_0^{r_m}\mathrm{d}\vec{r}\ [\rho_m g_0(r) + \omega_0^{\mathrm{nb}}(r)]} \quad (32)$$

for $r \le r_m$. The energy in eq 31 can then be expressed as

$$\langle V_N^{(1)}\rangle_0 = \frac{1}{2}nN\cdot h_z\int_0^{r_m} \mathrm{d}\vec{r}\ u^{(1)}(r)P_1(r) + \ldots = \frac{1}{2}nN\cdot h_z\langle u^{(1)}(r)\rangle_1 + \ldots \quad (33)$$

where $\langle u^{(1)}(r)\rangle_1$ is the average perturbed potential for the first shell. It is reasonably correct that we can equate $\langle u^{(1)}(r)\rangle_1$ to $u^{(1)}(r_e)$, so

$$\langle V_N^{(1)}\rangle_0 = \frac{1}{2}nN\int \mathrm{d}\vec{r}\ u^{(1)}(r)[\rho_m g_0(r) + \omega_0^{\mathrm{nb}}(r)] = \frac{1}{2}nN\cdot h_z u^{(1)}(r_e) + \ldots \quad (34)$$

The leading term in eq 34 is indeed the average packing energy $\langle U\rangle$ in eq 29.

The average perturbation energy $\langle V_N^{(1)}\rangle_0$ is still affected by higher coordination shells, though weakly so. The contribution from higher coordination shells is attractive. The perturbation energy will, however, be truncated after the first shell, which implies that the truncated perturbation energy is taken in the object function in eq 27 to fit the experimental bulk data. The characteristic temperature parameter, which is the phenomenological analog of the potential depth ϵ, will reflect the additional non-nearest neighbor effects. The truncation of the perturbation energy is roughly equivalent to a proper increase of ϵ.

Inserting the Mie potential in eq 11 into eq 34 yields

$$\langle V_N^{(1)}\rangle_0 = \frac{1}{2}nN\cdot h_z\epsilon f_P\left[\left(\frac{\sigma}{r_e}\right)^p - \left(\frac{\sigma}{r_e}\right)^6\right] \quad (35)$$

Recognizing the first shell as the building block of a given liquid, the most probable distance r_e would be related to the volume (v) per each monomer in some way. It is assumed, therefore, that

$$v \equiv \frac{V}{nN} \approx \gamma {r_e}^3 \quad (36)$$

where γ is a geometric constant. Equation 35 now becomes

$$\langle V_N^{(1)}\rangle_0 = \frac{1}{2}nN\cdot h_z\epsilon f_p\left[\gamma^{p/3}\left(\frac{\sigma^3}{v}\right)^{p/3} - \gamma^2\left(\frac{\sigma^3}{v}\right)^2\right] \quad (37)$$

The new energy parameter $\bar{\epsilon}$ is defined as $h_z\epsilon$. The reduced energy can then be written as

$$\frac{\langle V_N^{(1)}\rangle_0}{nN\bar{\epsilon}} = \frac{1}{2}f_p\left[\gamma^{p/3}\left(\frac{\sigma^3}{v}\right)^{p/3} - \gamma^2\left(\frac{\sigma^3}{v}\right)^2\right] = \frac{1}{2}f_p[(\gamma/C)^{p/3}\eta^{p/3} - (\gamma/C)^2\eta^2] \quad (38)$$

The last equality comes from the definition of the packing fraction. The symbol C, which is $\pi/6$, stands for the conversion factor of v into the packing fraction η.

In a general sense, the number of nonbonded mers, h_z, would have a slight density dependence. Because our primary concern is the dense liquid of long-chain molecules, h_z will be treated as constant throughout the following discussion. Along with the proposed relationship in eq 36, it is an artifact of this model that all the density dependence in the perturbation energy is concentrated on eq 36.

Combining eqs 24 and 38 yields the following complete free energy

$$\frac{\beta A}{nN} = \frac{3}{2}\left[\frac{1}{(1-\eta)^2} - \left(1 - \frac{1}{n}\right)\frac{1}{1-\eta}\right] - \frac{1}{n}\left[\ln(1-\eta) + \frac{3}{2}\right] + \frac{1}{n}\ln\frac{6\eta I\Lambda^{3n}}{\pi n\sigma^3 qe} + \frac{1}{2}f_p\beta\bar{\epsilon}[(\gamma/C)^{p/3}\eta^{p/3} - (\gamma/C)^2\eta^2] \quad (39)$$

Many important thermodynamic properties can be derived from eq 39. Prior to this, the three characteristic parameters should be defined. The basic parameters for chain molecules are the mer size σ, the potential depth ϵ, and the chain size n. However, the usual fitting procedure produces the phenomenological characteristic volume V^*, temperature T^*, and energy E^*. These parameters are defined for the current model as

$$V^* = \text{total hard core volume} = nN(\pi/6)\sigma^3$$
$$T^* = \bar{\epsilon}/k \quad (40)$$
$$E^* = nN\bar{\epsilon}$$

The characteristic pressure P^*, defined as E^*/V^*, is more often obtained instead of E^*. In the off-lattice

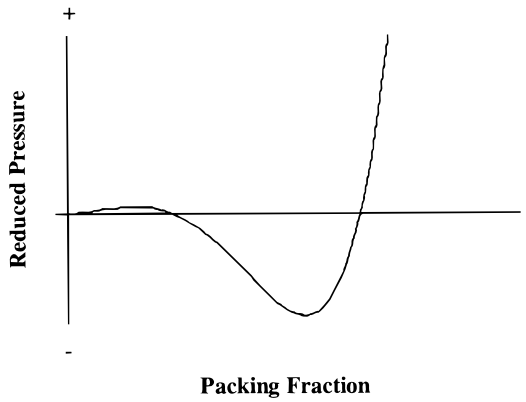

Figure 2. The schematic diagram of one selected isotherm from eq 42 for a moderately large chain length n. It is seen that eq 42 is basically a cubic equation of state. One can find three packing fractions at low pressures. These three packing fractions are for the vapor, liquid phases, and the region of instability. The vapor phase packing fraction can be suppressed if the chain length n is taken to ∞.

equation of state approach, the packing fraction is more commonly used than the reduced volume. The reduced volume is simply the inverse of the total packing fraction η:

$$\tilde{V} = \frac{V}{V^*} = \frac{V}{nN(\pi/6)\sigma^3} = \frac{v}{(\pi/6)\sigma^3} = \frac{1}{\eta} \qquad (41)$$

All the prerequisites have been defined and developed so far. A detailed analysis of the properties of the newly introduced free energy including a model-based interpretation of the $T-P$ superposition will be given in the following sections.

Characteristic Parameters for Polymers

To utilize the developed model for any other thermodynamic calculations, one requires the three characteristic parameters V^*, T^*, and P^*. These parameters are determined by fitting the experimental volumetric data to the following equation of state

$$\tilde{P} = \frac{P}{P^*} = -\frac{1}{P^*}\frac{\partial A}{\partial V}\Big)_T = \frac{T}{T^*}\left[\frac{3}{2}\frac{(\eta^2+\eta^3)}{(1-\eta)^3} + \frac{\eta}{n}\frac{(1+\eta/2)}{(1-\eta)^2}\right] + \frac{f_p}{2}\left[\frac{p}{3}(\gamma/C)^{p/3}\eta^{p/3+1} - 2(\gamma/C)^2\eta^3\right] \qquad (42)$$

An isotherm from eq 42 is shown schematically in Figure 2. This plot is similar to that from any known cubic equations of state. One can find the three packing fractions at best at a given temperature and pressure. These three packing fractions are for the vapor, liquid phases, and the region of instability. If one takes the chain length n to ∞, there remains only one packing fraction for the liquid phase.

Any nonlinear regression routine can be employed for the data reduction procedure. The geometric constant γ in eq 36 is a prerequisite for parameter estimation. Our choice is adopting $\gamma = 1/\sqrt{2}$ from the face-centered cubic lattice. Table 1 shows the characteristic parameters for 25 common polymers. In this table, we only included polymers with the tabulated raw bulk data. The overall average deviation between the experimental and the calculated volume is 0.0009 cm^3/g. The repulsive potential exponent p is set to be 12, which gives the Lennard−Jones (L−J) potential. In this case, the prefactor f_p in eq 12 becomes 4, as usual. Rodgers[37] collected all the characteristic parameters for six commonly used polymer equations of state including various cell models,[5−8,12] the hole model,[9] and the lattice fluid model.[10,11] Comparing the average deviation just given with those for other six models (0.0006 cm^3/g for the modified cell model[12] to 0.0033 cm^3/g for the lattice fluid model[10,11]) shows that the current model provides an excellent fitting performance.

It is natural to ask the size of a mer in this model. From the definition of the characteristic parameters, either the mer size σ or the number of repeating units in a mer can be calculated. The size σ of a mer is obtained by the relationship $T^*/P^* = (\pi/6)\sigma^3/k$. Table 1 gives the calculated sizes of mers for various polymers. It is noticeable that the model mer sizes are uniform with the average of 3.63 ± 0.22 Å. We can also measure the number of chemical repeating units, x/n, in a mer, if we denote x as the average degree of polymerization. It can be easily shown that

$$x/n = \frac{\mathrm{MW}}{\mathrm{MW}_r}\frac{1}{n} = \frac{kT^*}{\mathrm{MW}_r P^* V^*} \qquad (43)$$

These values are also tabulated in Table 1. For linear polyethylene (LPE) as an example, $x/n = 0.94$. This result implies that the model mer is close to the chemical repeating unit $-(CH_2)_2-$. One might notice that this mer size (≈3.4 Å) is small. The van der Waals volume of $-(CH_2)_2-$ is 20.5 cm^3/mol.[38] Equating this to $(\pi/6)N_A\sigma^3$, where N_A is Avogadro's number, $\sigma \approx 4.0$ Å. This discrepancy in the mer sizes implies that model mer size σ from V^* is unique to a given model. The σ from the model is not readily applicable to estimating the van der Waals volume of a given monomeric unit. The comparative study of mer sizes for different polymers is, however, possible.

The maximum packing fraction (η_{max}) of the current model is partially responsible for this relatively small model mer. The η_{max} is obtained at zero temperature and infinite pressure. From the vanishing average packing energy in eq 39, $\eta_{max} = C/\gamma = 0.74$. Meanwhile, the V^* of LPE is 0.479 cm^3/g. The specific volume of LPE melt up to 200 MPa lies between 1.16 and 1.4 cm^3/g. Therefore, the η of LPE lies between 0.35 and 0.4. The calculated packing fraction is rather low, it is 50−60% of the maximum packing fraction η_{max}. It is speculated that V^* may be increased if η_{max} is increased by taking different geometric constant γ. This low packing fraction can also be enhanced by taking more repulsive potential with greater p values. This procedure will be demonstrated in a later section.

The temperature parameter T^* is defined as $h_z\epsilon/k$. The number of nonbonded mers, h_z, is ∼10 when the total number of nearest neighbor mers equals 12. This difference results because we have to subtract 2 for the two bonded mers in calculating h_z. The potential depth ϵ/k can then be estimated. Because T^* of LPE is 2701.7 K, ϵ/k is close to 270 K, which is greater than ϵ/k of C_2H_4 (202.5 K) from the second virial coefficient data.[39] The estimated ϵ is qualitatively reasonable because the parameter ϵ/k contains the effects of the higher coordi-

Table 1. Characteristic Parameters, Monomer Sizes (σ), and the Number of Chemical Repeating Units (x/n) in a Monomer for the Current Model with the Lennard−Jones Potential ($p = 12$)

polymer	V^* (cm^3/g)	T^* (K)	P^* (MPa)	σ (Å)	x/n	$\langle\|\Delta V\|\rangle$ ($\times 10^4$ cm^3/g)^z
PS[a]	0.41857	4107.0	1644.0	4.04	0.48	6.9
PoMS[b]	0.42304	4024.7	1738.2	3.94	0.39	6.8
PVAc[c]	0.34786	2778.2	2149.2	3.24	0.36	1.2
PMMA[d]	0.36018	3645.6	2151.3	3.55	0.39	2.3
PcHMA[e]	0.39103	3736.0	1742.8	3.84	0.27	10.9
PnBMA[f]	0.40499	3184.8	1800.0	3.60	0.26	17.7
BPE[g]	0.49754	3023.4	1541.9	3.73	1.17	14.1
LPE[h]	0.47907	2701.7	1781.5	3.42	0.94	10.9
PIB[i]	0.48000	3849.3	1585.7	4.00	0.75	4.8
PDMS[j]	0.41325	2386.9	1083.2	3.87	0.60	8.0
PTFE[k]	0.18108	2167.9	1545.8	3.33	0.64	9.0
PBD[l]	0.47601	3251.1	1819.2	3.61	0.58	5.0
PEO[m]	0.37307	2875.0	2061.5	3.33	0.71	5.2
PTHF[n]	0.43311	3090.5	1632.7	3.68	0.50	7.1
PVME[o]	0.42179	3397.4	1814.5	3.67	0.64	14.6
PMA[p]	0.36497	3243.0	2095.6	3.44	0.41	15.6
PEMA[q]	0.37502	3088.7	2147.8	3.36	0.28	9.8
PEA[r]	0.37901	3077.2	1787.0	3.57	0.38	19.1
PECH[s]	0.32360	3922.9	2034.2	3.70	0.54	6.8
PCL[t]	0.40194	3600.8	1699.4	3.82	0.38	6.9
PVC[u]	0.31448	3982.8	1975.9	3.76	0.85	5.2
a-PP[v]	0.48440	2857.0	1382.5	3.79	0.82	10.2
TMPC[w]	0.36904	3170.7	1834.6	3.57	0.13	10.2
HFPC[x]	0.26472	2880.9	1883.8	3.43	0.13	7.3
BCPC[y]	0.29648	3507.6	2192.2	3.48	0.15	6.0

[a] Polystyrene.[49] [b] Poly(*o*-methyl styrene).[49] [c] Poly(vinyl acetate).[50] [d] Poly(methyl methacrylate).[51] [e] Poly(cyclo hexyl methacrylate).[51] [f] Poly(*n*-butyl methacrylate).[51] [g] Branched polyethylene.[51] [h] Linear polyethylene.[51] [i] Polyisobutylene.[52,53] [j] Polydimethylsiloxane.[53,54] [k] Polytetraflouro ethylene.[55] [l] Polybutadiene.[56] [m] Poly(ethylene oxide).[37] [n] Polyteterahydrofuran.[37] [o] Poly(vinyl methyl ether).[37] [p] Poly(methyl acrylate).[37] [q] Poly(ethyl methacrylate).[37] [r] Poly(ethyl acrylate).[37] [s] Polyepichlorohydrin.[37] [t] Polycarpolactam.[37] [u] Polyvinyl chloride.[37] [v] *a*-Polypropylene.[37] [w] Tetramethyl polycarbonate.[57] [x] Hexafluoro polycarbonate.[57] [y] Bischloro polycarbonate.[57] [z] The average deviation $\langle|\Delta V|\rangle \times 10^4$ in cm^3/g between the experimental data and the calculated value.

nation shells on the internal energy, which are attractive and tend to increase the theoretical ϵ/k.

Temperature−Pressure Superposition Principle

The main goal of this study is to understand the principle of $T-P$ superposition in the molecular point of view. We focus on the free energy asymmetry number B_1 ($=\partial B/\partial P)_{T|P\to 0}$), where B is the bulk modulus defined as $-\ v\partial P/\partial v)_T$. This parameter B_1 was shown to be temperature insensitive.[15,16]

The free energy in eq 39 along with eq 38 can be written succinctly as

$$\frac{A}{nN} = \frac{D_r}{v^{p/3}} - \frac{D_a}{v^{m/3}} + \frac{A_0}{nN} \tag{44}$$

where D_r and D_a are simply given by the combinations of $\bar{\epsilon}$, σ, and γ. The exponent m for the attractive potential is 6. Pressure is easily obtained by using the following standard thermodynamic relationships

$$P = -\left.\frac{\partial A/nN}{\partial v}\right)_T = \frac{(p/3)D_r}{v^{p/3+1}} - \frac{(m/3)D_a}{v^{m/3+1}} - \frac{A_{0,v}}{nN} \tag{45}$$

where the subscript v in the reference free energy implies its volume derivative. The bulk modulus B is then equal to

$$B = \frac{(p/3)(p/3+1)D_r}{v^{p/3+1}} - \frac{(m/3)(m/3+1)D_a}{v^{m/3+1}} + v\frac{A_{0,vv}}{nN} \tag{46}$$

The first pressure derivative of B can be obtained from eq 46 as

$$\left(\frac{\partial B}{\partial P}\right)_T = (p/3 + m/3 + 2) - (p/3+1)(m/3+1)\frac{P}{B} - \frac{1}{B}E\left(\frac{A_{0,v}}{nN}\right) \tag{47}$$

where the new functional $E(A_{0,v}/nN)$ is defined as

$$E\left(\frac{A_{0,v}}{nN}\right) \equiv v^2\frac{A_{0,vvv}}{nN} + [(p/3+1) + (m/3+1) + 1]v\frac{A_{0,vv}}{nN} + (p/3+1)(m/3+1)\frac{A_{0,v}}{nN} \tag{48}$$

The corresponding zero pressure value of eq 47 gives

$$B_1 = (p/3 + m/3 + 2) - \frac{1}{B_0}E\left(\frac{A_{0,v}}{nN}\right)\Big|_{P\to 0} \tag{49}$$

The newly introduced functional E greatly simplifies the free energy asymmetry number B_1.

Equation 49 shows that the leading expression for B_1 is from the Mie potential exponents p and m (= 6). Note that the remaining term in eq 49 is divided by the zero pressure bulk modulus B_0. Therefore, B_1 would be given dominantly by the leading term in eq 49, if B_0 is large enough. Figure 3 shows B_1 for the current model with $p = 12$ (L−J). Most polymers fall within the reduced temperature range shown in Figure 3. As can be seen in this figure, the variation of B_1 in this temperature range is within a few percent, which implies the temperature insensitiveness of B_1. The behavior of B_1 holds for greater p values (15 and 18 tested), as is also

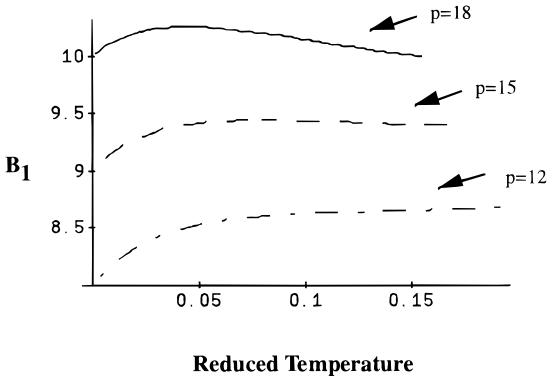

Figure 3. The theoretical free energy asymmetry number B_1 for the proposed model with the three Mie potential exponent p values.

shown in Figure 3. Therefore, the current model supports the empirical principle of $T-P$ superposition.

The average packing energy is based on the locally packed structure in the liquid state. The model free energy with the packing energy as a perturbation exhibits the temperature insensitiveness of the governing compression parameter B_1. The main contribution to B_1 comes from the packing energy, specifically from its exponents p and m (= 6). It was already mentioned that the compression parameter B_1 implies the shape of the free energy. The shape of the free energy is then exclusively described by the packing energy exponents. Therefore, the shape of the free energy is temperature insensitive.[40]

Maximum of Internal Pressure at Zero Pressure

It is also of our interest to understand the shape of the internal pressure P_i ($\equiv \partial U/\partial V)_T$). The P_i is in general given by the difference between the thermal pressure $T\alpha B$ and the system pressure P. The symbol α implies the thermal expansion coefficient. The P_i is known to be closely related to the strength of intermolecular interaction.[38,41−43] The internal pressure at zero pressure, $P_{i,0}$, is then equated to $T\alpha_0 B_0$, where the subscript 0 implies the zero pressure condition, which implies that $P_{i,0}$ vanishes at zero temperature. Because $P_{i,0}$ is positive and also vanishes at infinite temperature, $P_{i,0}$ should pass through a maximum at a certain temperature. An empirical investigation of such behavior of the internal pressure was recently given by the present authors.[17]

Figure 4 shows the internal energy U and the associated zero pressure volume for LPE from the current model with $p = 12$. The theoretical internal pressure $P_{i,0}$ for LPE at zero pressure from the current model is shown in Figure 5. It is easily seen that $P_{i,0}$ at the inflection point of U shows a maximum. From a molecular point of view, the temperature or volume at which the internal pressure has a maximum is regarded as the starting point where the repulsion between monomers in the system takes over the attraction. The current model takes the repulsion in the system into account via the packing energy. Therefore, the model exhibits the maximum of $P_{i,0}$.[44]

The experimental $P_{i,0}$ of LPE shown in Figure 5 suggests that its maximum is not seen in the normal liquid range of LPE. This result is so for many of other polymers.[17,41,42] However, the bulk data of poly(*n*-butyl methacrylate) (PnBMA) exhibits this phenomenon, as shown in Figure 6. These results are not contradicting,

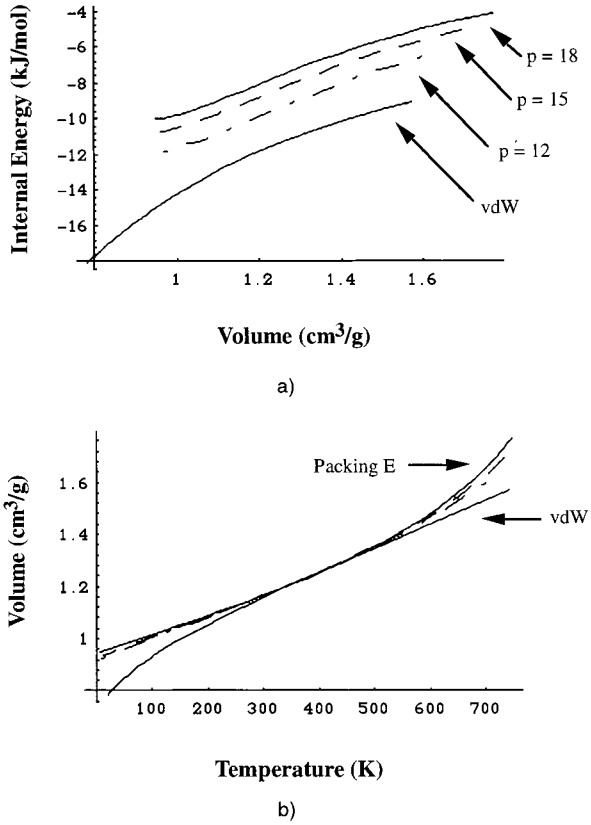

Figure 4. (a) The calculated internal energy of linear polyethylene from the proposed model with the packing energy as a function of volume. That from the van der Waals (vdW) fluid is also given. (b) The calculated volume at atmospheric pressure as a function of temperature. The volume in (a) can then be converted into temperature by using (b). Note that for three p values, the isobars are almost the same. The isobar from the proposed model is practically identical to that from the vdW fluid in the useful temperature range.

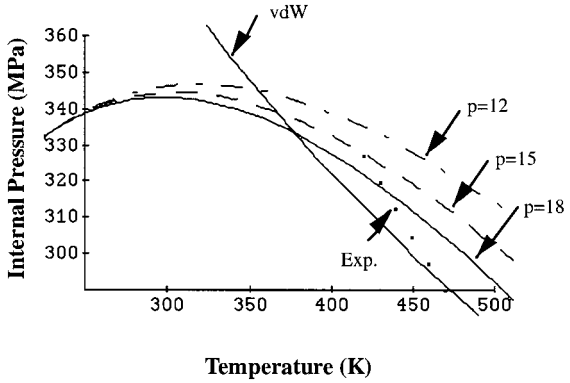

Figure 5. The comparison of the calculated internal pressure P_i of linear polyethylene at atmospheric pressure with the experimental one (ref 51). The P_i from the proposed model shows the maximum at a moderate temperature (325 K for p = 12 to 290 K for p = 18). The monotonically decreasing P_i from the van der Waals (vdW) fluid is also shown here.

even if the behavior of PnBMA is not common. Even for polymers that do not reveal the predicted maximum of $P_{i,0}$, we have suggested in our previous work that $P_{i,0}$ meet its maximum when the liquid data is extended to a lower temperature region.[17]

The experimental $P_{i,0}$ of PnBMA passes through a maximum at ~330 K.[45] For the L−J potential (p = 12), however, the theoretical maximum of $P_{i,0}$ is located at rather a higher temperature (at ~380 K for PnBMA)

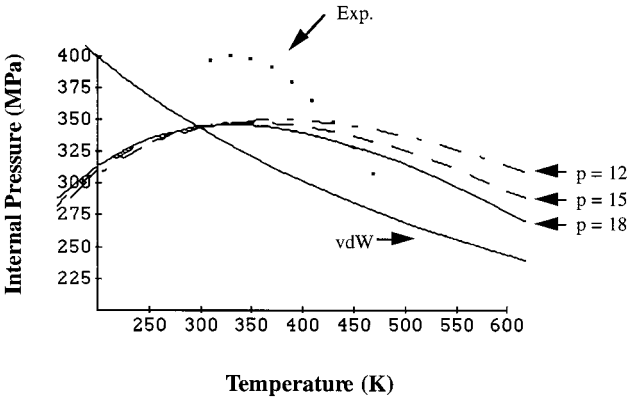

Figure 6. The comparison of the calculated internal pressure P_i of Poly(*n*-butyl methacrylate) at atmospheric pressure with the experimental one (ref 51). Both the theoretical and experimental P_i values exhibit the maxima. For the current model with $p = 12$, the maximum is located at $T \approx 380$ K. The experimental data and the model with $p = 18$ have the maxima at ~330 K.

than desired, which is indeed a general aspect of the current model with $p = 12$. In the next section, we deal with how to resolve such an undesirable feature of the model.

Toward a More Repulsive Potential

Michels et al.[46] performed a careful investigation on the second virial coefficient of argon. It was shown that the L−J potential was not completely satisfactory in describing the experimental second virial coefficient. The choice of the L−J potential is then a matter of convenience.

We allow the potential exponent p to be more repulsive than 12 (L−J) by taking 15 or 18. The potential with a greater p yields several interesting features. The characteristic parameters and the mer size σ of LPE for $p = 12$, 15, and 18 are compared in Table 2. It is evident that mer size σ and V^* become greater as the exponent p increases. The packing fraction η also increases as V^* increases. For $p = 18$, η is enhanced to 0.4−0.45 for LPE. The complete set of characteristic parameters for 25 polymers used before is tabulated in Table 3 in the case of $p = 18$ for reference purposes.

The maximum of $P_{i,0}$ is shifted toward a lower temperature region, as is shown in Figures 5 and 6. For PnBMA in Figure 6, the current model with $p = 18$ has the maximum of $P_{i,0}$ at almost the same temperature as the experimental one. In addition, adopting a greater p lends to improvement in the bulk data correlation.[47] Such results are shown in Table 4. A more repulsive potential than the L−J potential seems to improve the model to quite an extent.

The role of the Mie potential exponent p determines the shape of the potential. Taking a greater p gives a potential with a shorter ranged attraction and a steeper repulsion than the L−J potential. Such a shape of the potential was indeed suggested as a better description of the interparticle potential for noble gases.[19] The bulk data correlation of polymeric liquids seems to be compatible with the suggested shape of the interparticle potential.

Table 2. Comparison of Characteristic Parameters and Other Related Parameters of Linear Polyethylene for the Model with Varying Exponent p[a]

exponent p	V^* (cm^3/g)	T^* (K)	P^* (MPa)	σ (Å)	x/n	$\langle\|\Delta V\|\rangle$ ($\times 10^4$ cm^3/g)
12	0.47907	2701.7	1781.5	3.42	0.94	10.9
15	0.50727	2977.6	1515.6	3.73	1.15	7.2
18	0.53025	3255.4	1343.5	4.00	1.36	4.3

[a] $f_p = 4$, 3.07, and 2.60 for $p = 12$, 15, and 18, respectively.

Table 3. Characteristic Parameters, Monomer Size σ, and Ratio x/n of the Experimental Degree of Polymerization to the Theoretical One for the Proposed Model with the Repulsive Exponent $p = 18$[a]

polymer	V^* (cm^3/g)	T^* (K)	P^* (MPa)	σ (Å)	x/n	$\langle\|\Delta V\|\rangle$ ($\times 10^4$ cm^3/g)
PS	0.45666	4639.2	1201.9	4.67	0.68	4.6
PoMS	0.46304	4624.4	1277.9	4.57	0.55	4.9
PVAc	0.38172	3238.5	1639.4	3.73	0.50	0.9
PMMA	0.39436	4196.8	1590.1	4.11	0.56	1.5
PcHMA	0.42746	4267.0	1286.9	4.44	0.38	8.9
PnBMA	0.44228	3633.9	1356.4	4.13	0.35	12.6
BPE	0.54689	3545.2	1153.2	4.33	1.67	9.6
LPE	0.53025	3255.4	1343.4	4.00	1.36	4.3
PIB	0.52145	4246.2	1170.2	4.57	1.03	3.4
PDMS	0.45165	2737.8	829.1	4.43	0.82	5.9
PTFE	0.20921	2885.5	1201.3	3.99	0.95	6.4
PBD	0.51631	3540.3	1310.5	4.15	0.81	3.6
PEO	0.41166	3435.4	1600.5	3.84	0.99	3.6
PTHF	0.47449	3579.2	1248.7	4.23	0.70	4.6
PVME	0.45830	3780.1	1370.5	4.17	0.86	8.0
PMA	0.39835	3698.4	1599.9	3.94	0.56	10.1
PEMA	0.40996	3544.0	1638.9	3.85	0.38	8.6
PEA	0.41409	3528.4	1361.2	4.09	0.52	11.6
PECH	0.35091	4285.5	1502.5	4.22	0.73	4.6
PCL	0.43644	3972.6	1265.3	4.36	0.52	4.6
PVC	0.34289	4481.9	1444.2	4.34	1.20	4.3
a-PP	0.53016	3295.4	1057.7	4.35	1.14	7.0
TMPC	0.40952	3856.8	1397.4	4.17	0.18	7.7
HFPC	0.29359	3498.8	1441.8	4.00	0.19	5.1
BCPC	0.32633	4140.6	1665.4	4.03	0.21	5.0

[a] Polymer names and the cited references are the same as in Table 1.

Table 4. Overall Average Deviation Between the Experimental Volumetric Data of Polymers Used in Table 1 and the Model with Varying Exponent *p* Compared With the van der Waals (vdW) Fluid

	current model			vdW
exponent	$p = 18$	$p = 15$	$p = 12$ (L−J)	fluid
avg. deviation[a] ($\times 10^4$ cm^3/g)	6.1	7.4	8.9	9.9

[a] Average deviation $\langle|\Delta V|\rangle \times 10^4$ in cm^3/g for 25 polymers.

Table 5. Comparison of the Calculated Cohesive Energies of Linear Polyethylene at 298 K for the Current Model and the van der Waals (vdW) Fluid

	current model			vdW
exponent	$p = 18$	$p = 15$	$p = 12$ (L−J)	fluid
cohesive energy (kJ/mol)	8.4	9.1	10.2	12.3

The cohesive energy (CE) is a property that may demonstrate this shape effect of the interparticle potential. The CE is simply the negative of internal energy in Figure 4a. The experimental CE value of LPE at 298 K is 8.7 ± 0.4 kJ/mol.[38,48] The CE of LPE calculated from the current model with three *p* values at 298 K is shown in Table 5. The data indicate that there are marked differences in the theoretical CE values. The CE from the current model with $p = 18$ is 8.4 kJ/mol, which is within the experimental range. As *p* decreases to 12, the model gradually overestimates the CE. The more repulsive potential better describes the experimental CE than the conventional L−J potential. The reason for this better description is the difference in the range of the perturbed interaction. The shorter interaction tail of the more repulsive potential gives the diminished cohesion in the system, as shown in Figure 4a.

Comparison with the van der Waals Energy as a Perturbation

The simplest perturbation energy can be given by the mean field van der Waals (vdW) energy that is proportional to the global packing fraction η. The free energy of the vdW fluid (hard chain reference free energy + vdW energy) is identical to eq 39 except that the whole energy term is replaced with $U_{vdW} = -nN\bar{\epsilon}\eta$, where $\bar{\epsilon}$ here is a proper interaction parameter for the vdW energy. The characteristic parameters V^*, T^*, and P^* can be defined as before. For reference purposes, we tabulated in Table 6 the characteristic parameters of the vdW fluid for the whole compendium of polymers. The fitting performance of the vdW fluid is comparable with the current model with $p = 12$ (L−J). Indeed, 0.0010 cm^3/g is the overall average deviation between the experimental volumetric data and the vdW fluid for 25 polymers used here.

The vdW energy ignores any local structure in given polymer liquids. It then loses information on the interparticle potential. Therefore, any relationship between the free energy asymmetry number B_1 and the nature of the interparticle potential is not expected from the vdW fluid. The vdW fluid, as a result, provides no clue to the $T-P$ superposition principle. The current model with $p = 18$ supports the $T-P$ superposition principle. The accuracy of the current model with $p = 18$, therefore, surpasses that of the vdW fluid, as is seen in Table 4.

The vdW fluid does not exhibit the maximum of the internal pressure, as is illustrated in Figures 5 and 6. This effect will then yield the internal energy behaving differently from the experimental one when temperature is lowered. The CE of LPE calculated from the vdW fluid along with those from the current model with varying *p* values at 298 K is shown in Table 5. In the vdW energy, there is no repulsion taken into account. Therefore, the CE continues to increase as temperature is lowered. One can read 12.3 kJ/mol as the CE of the vdW fluid. Therefore, the packing energy yields a CE closer to the experimental one than does the vdW fluid because the packing energy is shorter ranged than the vdW energy and because the repulsion in the system is taken into consideration in the packing energy.

Table 6. Characteristic Parameters, Monomer Size σ, and Ratio x/n of the Experimental Degree of Polymerization to the Theoretical One for the van der Waals (vdW) Fluid[a]

polymer	V^* (cm^3/g)	T^* (K)	P^* (MPa)	σ (Å)	x/n	$\langle|\Delta V|\rangle$ ($\times 10^4$ cm^3/g)
PS	0.60170	15741.0	775.1	8.12	2.70	6.9
PoMS	0.60499	15121.5	871.8	7.70	2.02	4.7
PVAc	0.48416	9292.2	1284.1	5.76	1.44	1.6
PMMA	0.50812	12882.1	1156.3	6.65	1.82	3.0
PcHMA	0.55267	13252.1	900.2	7.29	1.32	10.7
PnBMA	0.56742	10844.0	969.0	6.66	1.15	18.0
BPE	0.67227	8952.8	972.7	6.24	4.07	11.9
LPE	0.62759	7204.2	1286.1	5.29	2.65	6.8
PIB	0.70525	16561.6	701.3	8.54	4.97	4.5
PDMS	0.56772	7539.9	650.7	6.74	2.29	7.6
PTFE	0.27089	6525.0	515.3	6.94	3.89	36.4
PBD	0.69293	13065.5	747.5	7.72	3.88	11.0
PEO	0.49851	8207.5	1438.7	5.32	2.16	9.6
PTHF	0.60342	10360.4	962.7	6.57	2.06	8.8
PVME	0.59945	12301.9	905.0	7.10	3.25	14.5
PMA	0.51020	10959.3	1158.4	6.30	1.79	16.1
PEMA	0.51792	9957.8	1259.2	5.93	1.11	9.8
PEA	0.52596	10070.5	1007.7	6.41	1.58	20.3
PECH	0.47274	16269.4	882.8	7.86	3.50	5.0
PCL	0.57084	12964.3	832.6	7.43	1.99	5.3
PVC	0.45537	15840.1	912.9	7.71	5.07	4.7
a-PP	0.67121	9359.9	815.0	6.72	3.31	7.7
TMPC	0.48198	8378.9	1356.0	5.46	0.34	9.2
HFPC	0.33837	7112.2	1483.9	5.02	0.33	7.3
BCPC	0.39884	10241.2	1440.3	5.72	0.48	6.6

[a] Polymer names and the cited references are the same as in Table 1.

Summary

A new analytical equation of state model for nonpolar polymers has been formulated to provide a better understanding of the empirical $T-P$ superposition principle. Upon the simplification of a chain as interacting tangent spheres, a perturbation method is employed to obtain a free energy. Nonbonded monomers interact with others with the hard reference potential and the attractive perturbed potential. The Mie potential with the repulsion exponent p is chosen as the perturbed attractive potential. The Mie potential exponent p from 12 (L−J) to 18 is taken into consideration.

In the context of the perturbation theory, the free energy is divided into the reference free energy and the perturbation energy. The reference free energy was obtained by considering the configurational partition function of the hard chain system at infinite dilution in combination with the Baxter−Chiew hard chain equation of state. The average packing energy is adopted as a perturbation energy for the description of the dense polymeric liquids. The packing energy represents the local packing in polymeric liquids, which is primarily responsible for compression.

The current model requires three molecular parameters: monomer size σ, interaction parameter ϵ, and the chain size n. These molecular parameters are tabulated for commonly used polymers in case of the L−J potential ($p = 12$) chosen as the perturbed potential. The theoretical equation of state shows an excellent fitting performance when compared with the experimental volumetric data of common polymers. The accuracy of the model improves as the more repulsive potential ($p > 12$) is taken as the perturbed potential.

The most interesting feature of the model can be found in the analysis of the free energy asymmetry number B_1. This parameter is defined as the pressure derivative of the bulk modulus B at zero pressure. The model suggests that B_1 is dominantly described by the packing energy, especially by its Mie potential exponents. Therefore, B_1 is temperature insensitive and it determines the shape of the free energy, and the shape of the free energy is then temperature insensitive, which is the essence of the $T-P$ superposition of polymer compression. The proposed model supports the principle of $T-P$ superposition.

Another important feature of the model is the existence of the maximum of the internal pressure at zero pressure and a moderate temperature. The internal energy of the model takes the repulsion between nonbonded monomers into account via the packing energy. The maximum of the internal pressure occurs where the repulsion in the system starts to take over the attraction. This phenomenon, though not seen in the normal liquid range of many polymers, appears more evidently when analyzing the bulk data of PnBMA. For the L−J potential, the theoretical maximum of the internal pressure is located in rather a higher temperature region than desired. Temperature at which the maximum occurs is, however, lowered as the more repulsive potential is used as the perturbed potential.

The polymer bulk data correlation including the location of the internal pressure maximum and the cohesive energy calculation both favor to take the intermer potential with the more repulsive interaction. In particular, the model with the repulsive exponent $p = 18$ predicts the cohesive energy of linear polyethylene within the experimental range. The shape of such intermer potential is characterized by the shorter ranged attraction and the steeper repulsion than that of the conventional L−J potential.

Local packing primarily determines pressure in the polymeric liquid state. The simple packing energy well describes this local packing of nonbonded monomers. The obtained analytical free energy with the packing energy as a perturbation provides an accurate engineering fitting function of polymer bulk data. The model supports the desired properties of the $T-P$ superposition and the maximum of the internal pressure. These two properties originate in the properties of the shape of the packing energy. The former is given by the temperature insensitiveness of its shape. The latter is given by the volume dependence of its shape.

Acknowledgment. The authors acknowledge the financial support of the Korea Research Foundation made in the program year of 1997.

Appendix

Definitions of Various Distribution Functions. Single-chain and chain−chain distribution functions can be formally defined in the following way

$$\rho^{(1)}(\{\vec{r}_1\}) = \frac{N}{Z_N}\int e^{-\beta V_N}\prod_{i=2}^{N} d\{\vec{r}_i\}$$

$$\rho^{(2)}(\{\vec{r}_1\},\{\vec{r}_2\}) = \frac{N(N-1)}{Z_N}\int e^{-\beta V_N}\prod_{i=3}^{N} d\{\vec{r}_i\} \quad \text{(A1)}$$

The meaning of $\rho^{(1)}(\{\vec{r}_1\})\, d\{\vec{r}_1\}$ is the probability of finding a chain at $\{\vec{r}_1\}$ within the hyperdimensional rectangle $d\{\vec{r}_1\}$. Likewise $\rho^{(2)}(\{\vec{r}_1\},\{\vec{r}_2\})\, d\{\vec{r}_1\}\, d\{\vec{r}_2\}$ implies the probability of finding a chain at $\{\vec{r}_1\}$ within $d\{\vec{r}_1\}$ and another chain at $\{\vec{r}_2\}$ within $d\{\vec{r}_2\}$.

The intermolecular site−site distribution function $g^{(\alpha\gamma)}(r)$ is defined as

$$g^{(\alpha\gamma)}(r) \equiv \frac{1}{\rho^2}\int \rho^{(2)}(\{\vec{r}_1\},\{\vec{r}_2\}) \prod_{\substack{a\neq\alpha \\ a\geq 1}}^{n} d\vec{r}_1{}^{(a)} \prod_{\substack{b\neq\gamma \\ b\geq 1}}^{n} d\vec{r}_2{}^{(b)} \quad \text{(A2)}$$

where the superscript (a) or (b) indicates one of n-sites of chains. The ρ factor in eq A2 implies the bulk number density. This function represents the probability of finding two sites α and γ on different chains separated by $r = |\vec{r}_2{}^{(\gamma)} - \vec{r}_1{}^{(\alpha)}|$ regardless of other sites.

Because we are dealing with chains instead of particles, it is required to define the intramolecular site−site probability density function $\omega^{(\alpha\gamma)}(r)$ as

$$\omega^{(\alpha\gamma)}(r) \equiv \frac{1}{\rho}\int \rho^{(1)}(\{\vec{r}_1\}) \prod_{\substack{a\neq\alpha,\gamma \\ a\geq 1}}^{n} d\vec{r}_1{}^{(a)} \quad \text{(A3)}$$

The intramolecular probability $\omega^{(\alpha\gamma)}(r)$ implies the probability of finding two sites α and γ on the same chain separated by $r = |\vec{r}_1{}^{(\gamma)} - \vec{r}_1{}^{(\alpha)}|$.

The averaged distribution functions g and ω can also be defined as

$$g = \frac{1}{n^2}\sum_{\alpha,\gamma} g^{(\alpha\gamma)}$$

$$\omega = \frac{1}{n}\sum_{\alpha,\gamma} \omega^{(\alpha\gamma)} \tag{A4}$$

The average intramolecular distribution function of nonbonded pairs, $\omega^{nb}(r)$, can be defined similarly as

$$\omega^{nb}(r) \equiv \frac{1}{n}\sum_{|k-l|>1} \omega^{(kl)}(r) \tag{A5}$$

References and Notes

(1) Macdonald, J. R. *Rev. Mod. Phys.* **1969**, *41*, 316.
(2) Tait, P. G. *Phys. Chem.* **1888**, *2*, 1.
(3) Tammon, G. *Z. Phys. Chem.* **1895**, *17*, 620.
(4) Murnaghan, F. D. *Proc. Nat. Acad. Sci.* **1944**, *30*, 244.
(5) Prigogine, I.; Mathot, V. *J. Chem. Phys.* **1952**, *20*, 49.
(6) Prigogine, I.; Trappeniers, N.; Mathot, V. *Disc. Faraday Soc.* **1953**, *15*, 93.
(7) Prigogine, I.; Bellemans, A.; Mathot, V. *The Molecular Theory of Solutions*; North Holland: Amsterdam, Netherlands, 1957.
(8) Flory, P. J.; Orwoll, R. A.; Vrij, A. *J. Am. Chem. Soc.* **1964**, *86*, 3515.
(9) Simha, R.; Somcynsky, T. *Macromolecules* **1969**, *2*, 342.
(10) Sanchez, I. C.; Lacombe, R. H. *J. Phys. Chem.* **1976**, *80*, 2352.
(11) Sanchez, I. C.; Lacombe, R. H. *J. Polym. Sci., Polym. Lett. Ed.* **1977**, *15*, 71.
(12) Dee, G. T.; Walsh, D. J. *Macromolecules* **1988**, *21*, 815.
(13) Huang, S. H.; Radosz, M. *Ind. Eng. Chem. Res.* **1990**, *29*, 2284.
(14) Song, Y.; Lambert, S. M.; Prausnitz, J. M. *Ind. Eng. Chem. Res.* **1994**, *33*, 1047.
(15) Sanchez, I. C.; Cho, J.; Chen, W.-J. *J. Phys. Chem.* **1993**, *97*, 6120.
(16) Sanchez, I. C.; Cho, J.; Chen, W.-J. *Macromolecules* **1993**, *26*, 4234.
(17) Sanchez, I. C.; Cho, J. *Polymer* **1995**, *36*, 2929.
(18) McQuarrie, D. A. *Statistical Mechanics*; Harper & Row: New York, 1976.
(19) Hansen, J.-P.; McDonald, I. R. *Theory of Simple Liquids*; Academic: London, 1986.
(20) Percus, J. K.; Yevick, G. J. *Phys. Rev.* **1958**, *110*, 1.
(21) Baxter, R. J. *J. Chem. Phys.* **1968**, *49*, 2770.
(22) Barboy, B. *Chem. Phys.* **1975**, *11*, 357.
(23) Chiew, Y. C. *Mol. Phys.* **1990**, *70*, 129.
(24) Wertheim, M. S. *J. Stat. Phys.* **1984**, *35*, 19.
(25) Wertheim, M. S. *J. Stat. Phys.* **1984**, *35*, 35.
(26) Wertheim, M. S. *J. Stat. Phys.* **1986**, *42*, 459.
(27) Wertheim, M. S. *J. Stat. Phys.* **1986**, *42*, 477.
(28) Wertheim, M. S. *J. Chem. Phys.* **1987**, *87*, 7323.
(29) Chapman, W. G.; Jackson, G.; Gubbins, K. E. *Mol. Phys.* **1988**, *65*, 1057.
(30) Dickman, R.; Hall, C. K. *J. Chem. Phys.* **1986**, *85*, 4108.
(31) Honnel, K. G.; Hall, C. K. *J. Chem. Phys.* **1989**, *90*, 1841.
(32) Zwanzig, R. W. *J. Chem. Phys.* **1954**, *22*, 1420.
(33) Chan, H. S.; Dill, K. A. *J. Chem. Phys.* **1994**, *101(8)*, 7007.
(34) Barker, J. A.; Henderson, D. *J. Chem. Phys.* **1967**, *47*, 2856.
(35) Malakhov, A. O.; Brun, E. B. *Macromolecules* **1992**, *25*, 6262.
(36) Mitlin, V. S.; Sanchez, I. C. *J. Chem. Phys.* **1993**, *99*, 533.
(37) Rodgers, P. A. *J. Appl. Polym. Sci.* **1993**, *48*, 1061.
(38) van Krevlan, D. W. *Properties of Polymers*; Elsevier Science: Amsterdam, Netherlands, 1990.
(39) Prausnitz, J. M.; Lichtenthaler, R. N.; Gomez de Azevedo, E. *Molecular Thermodynamics of Fluid-Phase Equilibria*; 2nd ed.; Prentice-Hall: New Jersey, 1986.
(40) This temperature-insensitive shape of the theoretical free energy can be visualized by simply plotting the calculated compression strain, $\ln(V/V_0)$, at several temperatures as a function of the scaled pressure P/B_0. The V_0 here is the theoretical zero pressure isobar. Because the governing parameter for such plots is B_1, the temperature-insensitive B_1 from the theory would make the compression isotherms superposed into a single curve.
(41) Allen, G.; Gee, G.; Wilson, J. G. *Polymer* **1960**, *1(4)*, 456.
(42) Allen, G.; Gee, G.; Mangaraj, D.; Sims, D.; Wilson, G. J. *Polymer* **1960**, *1*, 467.
(43) Voeks, J. F. *J. Polym. Sci.: Part A* **1964**, *2*, 5319.
(44) A few quasilattice models[5−7,9,12] also show this maximum of $P_{i,0}$.
(45) We found another data set of liquid PnBMA that also exhibits the $P_{i,0}$ maximum at almost the identical temperature; see Zoller, P.; Walsh, D. *Standard Pressure-Volume-Temperature Data for Polymers*; Technomic: Lancaster, 1995.
(46) Michels, A.; Levelt, J. M.; DeGraff, W. *Physica* **1958**, *24*, 659.
(47) Some quasilattice models[5−7,9,12] give slightly better fitting performance than the present model with $p = 12$. By taking $p > 12$, the current model provides a performance comparable to that of those models.
(48) Brandrup, J.; Immergut, E. H. *Polymer Handbook*; John Wiley & Sons: New York, 1989.
(49) Quach, A.; Simha, R. *J. Appl. Phys.* **1971**, *42*, 4592.
(50) McKinney, J. E.; Goldstein, M. *J. Res. Nat. Bur. Stand.* **1974**, *78A*, 331.
(51) Olabisi, O.; Simha, R. *Macromolecules* **1975**, *8*, 206.
(52) Eichinger, B. E.; Flory, P. J. *Macromolecules* **1968**, *1*, 285.
(53) Beret, S.; Prausnitz, J. M. *Macromolecules* **1975**, *8*, 536.
(54) Shih, H.; Flory, P. J. *Macromolecules* **1972**, *5*, 758.
(55) Zoller, P.; Kehl, T. A.; Starkweather, H. W. J.; Jones, G. A. *J. Polym. Sci., Polym. Phys. Ed.* **1989**, *27*, 993.
(56) Barlow, J. W. *Polym. Eng. Sci.* **1978**, *18*, 238.
(57) Kim, C. K., Thesis, University of Texas at Austin, 1992.

MA971784C